

This is the peer reviewed version of the following article:

Probing magnetic coupling between LnPc<sub>2</sub> (Ln=Tb, Er) molecules and graphene / Ni(111) substrate with and without Au-intercalation: role of the dipolar field / Corradini, Valdis; Candini, Andrea; Klar, David; Biagi, Roberto; De Renzi, Valentina; Lodi Rizzini, Alberto; Cavani, Nicola; Del Pennino, Umberto; Klyatskaya, Svetlana; Ruben, Mario; Velez-Fort, Emilio; Kummer, Kurt; Brookes, Nicholas B.; Gargiani, Pierluigi; Wende, Heiko; Affronte, Marco. - In: NANOSCALE. - ISSN 2040-3364. - 10:1(2018), pp. 277-283. [10.1039/C7NR06610D]

*Terms of use:*

The terms and conditions for the reuse of this version of the manuscript are specified in the publishing policy. For all terms of use and more information see the publisher's website.

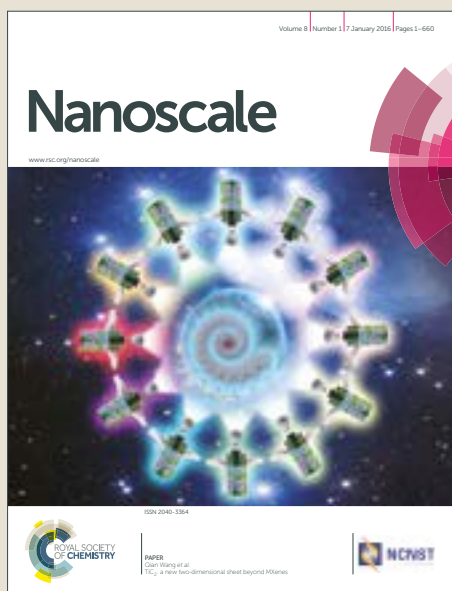
18/12/2025 19:40

# Nanoscale

Accepted Manuscript



This article can be cited before page numbers have been issued, to do this please use: V. Corradini, A. Candini, D. Klar, R. Biagi, V. de Renzi, A. Lodi Rizzini, N. Cavani, U. del Pennino, S. Klyatskaya, M. Ruben, E. Velez-Fort, K. Kummer, N. B. Brookes, P. Gargiani, H. Wende and M. Affronte, *Nanoscale*, 2017, DOI: 10.1039/C7NR06610D.



This is an Accepted Manuscript, which has been through the Royal Society of Chemistry peer review process and has been accepted for publication.

Accepted Manuscripts are published online shortly after acceptance, before technical editing, formatting and proof reading. Using this free service, authors can make their results available to the community, in citable form, before we publish the edited article. We will replace this Accepted Manuscript with the edited and formatted Advance Article as soon as it is available.

You can find more information about Accepted Manuscripts in the [author guidelines](#).

Please note that technical editing may introduce minor changes to the text and/or graphics, which may alter content. The journal's standard [Terms & Conditions](#) and the ethical guidelines, outlined in our [author and reviewer resource centre](#), still apply. In no event shall the Royal Society of Chemistry be held responsible for any errors or omissions in this Accepted Manuscript or any consequences arising from the use of any information it contains.



## Probing magnetic coupling between LnPc<sub>2</sub> (Ln=Tb, Er) molecules and graphene / Ni (111) substrate with and without Au-intercalation: role of the dipolar field

V. Corradini<sup>1</sup>, A. Candini<sup>1\*</sup>, D. Klar<sup>2</sup>, R. Biagi<sup>1,3</sup>, V. De Renzi<sup>1,3</sup>, A. Lodi Rizzini<sup>1,3,8</sup>, N. Cavani<sup>1,3</sup>, U. del Pennino<sup>1,3</sup>, S. Klyatskaya<sup>4</sup>, M. Ruben<sup>4,5</sup>, E. Velez-Fort<sup>6</sup>, K. Kummer<sup>6</sup>, N. B. Brookes<sup>6</sup>, P. Gargiani,<sup>7</sup> H. Wende<sup>2</sup>, M. Affronte<sup>1,3</sup>

<sup>1</sup>Centro S3, Istituto Nanoscienze - CNR, via G. Campi 213/A, 41125 Modena. Italy.

<sup>2</sup>Faculty of Physics and Center for Nanointegration Duisburg-Essen (CENIDE), University of Duisburg-Essen, Lotharstraße 1, D-47048 Duisburg, Germany

<sup>3</sup>Dipartimento di Scienze Fisiche, Matematiche e Informatiche, Università di Modena e Reggio Emilia via G. Campi 213/A, 41125/A Modena. Italy.

<sup>4</sup>Institute of Nanotechnology, Karlsruhe Institute of Technology (KIT), D-76344 Eggenstein-Leopoldshafen, Germany

<sup>5</sup>Institut de Physique et Chimie des Matériaux de Strasbourg, UMR 7504 UdS-CNRS, 67034 Strasbourg Cedex 2, France

<sup>6</sup>European Synchrotron Radiation Facility (ESRF), Avenue des Martyrs 71, 38043 Grenoble, France

<sup>7</sup>ALBA Synchrotron Light Source, E-08290 Barcelona, Spain

<sup>8</sup>CNR-IOM, Laboratorio TASC, Area Science Park, S.S. 14, km 163.5, 34012 Basovizza (Trieste), Italy

\* present affiliation: Istituto di Sintesi Organica e Fotoreattività (ISOF), Consiglio Nazionale delle Ricerche (CNR), Via Gobetti 101, 40129 Bologna, Italy

### ABSTRACT.

Lanthanides (Ln) bis-phthalocyanine (Pc), the so called LnPc<sub>2</sub> *double decker*, are promising class of molecules, with well-defined magnetic anisotropy. In this work, we investigate the magnetic properties of LnPc<sub>2</sub> molecules UHV-deposited on the graphene/Ni(111) substrate, and how they modify when an Au layer is intercalated between the Ni and graphene. X-ray absorption spectroscopy (XAS), linear and magnetic circular dichroism (XLD and XMCD) were used to characterize the systems and probe the magnetic coupling between LnPc<sub>2</sub> molecules and the Ni substrate through graphene, both gold intercalated or not. Two types of LnPc<sub>2</sub> molecules (Ln=Tb, Er) with a different magnetic anisotropy (easy-axis for Tb, easy-plane for Er) were considered. XMCD shows an antiferromagnetic coupling between Ln and

Ni(111) even in the presence of the graphene interlayer. Au intercalation causes the vanishing of the interaction between Tb and Ni(111). On the contrary, in the case of ErPc<sub>2</sub>, we found that the gold intercalation does not perturb the magnetic coupling. These results, combined with the magnetic anisotropy of the systems, suggests the possible importance of the magnetic dipolar field contribution in determining the magnetic behaviour.

## INTRODUCTION.

Molecules made of a magnetic core and an organic shell are recognized as promising moieties for exploiting magnetism at the nano-scale [01, 02, 03] and molecular spintronics. Transition metal porphyrins and phthalocyanines represent a prototypical class of molecules: they can be easily deposited in clean conditions and grow self-assembled ordered layers on metal surfaces [ref04]. More than a decade ago it was shown that these molecules couple magnetically on ferromagnetic substrates, by direct exchange or ligand-mediated superexchange interaction [05, 06, 07, 08, 09], but due to their paramagnetic behaviour they only mimic the substrate magnetization.

Along this line, the class of the lanthanides (Ln) bis-phthalocyanine (Pc), so called LnPc<sub>2</sub> *double decker*, have raised considerable interest, since they present the same versatility of the transition metal phthalocyanines and porphyrins, but behave as single molecule magnets (SMMs), retaining their magnetization below a certain blocking temperature [10, 11]. This magnetic nature derives from their morphology and electronic configuration: the magnetization of the *f*-shell Ln ions exhibits a well-defined magnetic anisotropy, as a consequence of the ligand field created by the two Pcs between which the magnetic ions are sandwiched. Furthermore, the neutral derivative [LnPc<sub>2</sub>]<sup>0</sup> possesses one unpaired electron that is delocalized in the phthalocyanines, making the molecules suitable to ligand-mediated interactions with the substrates [12].

TbPc<sub>2</sub> couples antiferromagnetically when deposited on a magnetic layer and behaves as an independent magnetic unit, given that its magnetization depends critically on the orientation of the molecule easy axis as well as on the interplay of ligand mediated super-exchange interaction with the substrate and the applied magnetic field [07]. In recent works, we have demonstrated that super-exchange interaction can couple the magnetic moment of the Ln to Ni substrates thanks to a partial overlap of the *d*-orbitals of the Ln (in turn, mediating the polarization of the inner *f*-shell electrons) with those of the Pc [13].

Super-exchange interaction between a magnetic substrate and 3d single atoms/clusters [14], transition metal phthalocyanines and porphyrins [15, 16, 17, 12] and  $\text{LnPc}_2$  SMMs [18] have been observed also when a graphene interlayer is present. In recent years, graphene has been widely studied for applications in the field of spin transport and spintronic devices [19], due to its properties such as high in-plane charge carrier mobility [20], low spin-orbit interaction and the capability to passivate metal (and magnetic) surfaces through weak Van der Waals interactions with the surface [21, 22]. It is therefore extremely interesting to investigate in details the role of a graphene layer in mediating the coupling between a magnetic substrate and the molecular moieties. We have recently shown, for the case of the  $\text{TbPc}_2$  molecules, how a graphene layer directly grown on Ni still allows super-exchange coupling through a relay-like mechanism mediated by the electron spin delocalized in the Pc ligands [18].

In the present work, we pursue this issue, investigating the presence or absence of magnetic coupling between a molecular probe and a graphene/Ni(111) substrate when an Au layer is intercalated between Ni and graphene. In this system, Au acts as a further spacer, increasing the distance between the ferromagnetic substrate and the molecules, but also changes the characteristics of the graphene layer. The most important effect is the decoupling of graphene from the Ni substrate, thus almost restoring its free-standing properties [23]. Moreover, the gold layer induces, through spin-orbit interaction, a significant spin splitting of the energy bands of graphene [24].

For our purposes we focus, as molecular probes, on two  $\text{LnPc}_2$  derivatives bearing a strong – but different- magnetic anisotropy [25].  $\text{TbPc}_2$  has a  $L=3$ ,  $S=3$ ,  $J=6$  ground state and the ligand field leads to a huge uniaxial anisotropy leaving the  $m_J=\pm 6$  doublet to behave as an Ising spin with the easy axis perpendicular to the planes of the two phthalocyanines.  $\text{ErPc}_2$  has a  $L=6$   $S=3/2$   $J=15/2$  ground state and the ligand field induces an in-plane anisotropy, leaving the  $m_J=\pm 1/2$  as the ground doublet.

After describing the preparation and characterization of the systems, we focus on the results of low temperature XMCD investigations. For the sake of completeness, we compare the molecule behaviour on graphene/Au/Ni with that observed when molecules are deposited directly on bare Ni(111) and on graphene/Ni(111), reported in previous works [13 18].

## EXPERIMENTAL

The single-layer graphene (SLG) was grown on the Ni(111) single-crystal substrate following

the procedure reported in literature [26,27,28]. Au intercalation was carried out by evaporating 0.5 nm of gold (monitored by a quartz microbalance and cross-checked by XPS) on the SLG/Ni(111) surface and subsequently annealing for 10 min at 430 °C as described in Ref [23,24]. The quality, homogeneity, and cleanliness of both SLG/Ni(111) and SLG/Au/Ni(111) were checked by LEED and by XPS (see fig.S1). In particular, after Au intercalation the C-1s shifts from 284.7 eV (strongly interacting graphene) to 284.3 eV ( $C_{Au}$ ), which corresponds to the non-interacting free-standing graphene. A further proof of the high quality of this interface is the measurement of the graphene  $\pi$ -band dispersion around the K point, performed by Angle-Resolved Photoemission Spectroscopy (ARPES) at the APE beamline of the ELETTRA Synchrotron Radiation Facility [29] and shown in Fig.S2 (see SI). These measurements confirm that the properties of freestanding graphene are restored by intercalation of an Au layer.

The X-ray Absorption Spectroscopy (XAS) experiments were carried out at the BOREAS beamline [30] of the ALBA Synchrotron Radiation Facility (Spain) and at the ID32 beamline [31] of the European Synchrotron Radiation Facility (ESRF) in Grenoble (France). Once introduced in the experimental chamber, the ex-situ prepared samples were annealed at 300°C for 5min to restore the SLG/Ni(111) and SLG/Au/Ni(111) surfaces. ~0.3 monolayer of LnPc<sub>2</sub> molecules (Ln=Tb, Er) was evaporated from well-outgassed powder evaporators, at a temperature of 420 °C and at a base pressure of  $1.0 \times 10^{-9}$  mbar. The evaporation rate and the film thickness were monitored through a calibrated quartz microbalance. The coverage was also cross-checked in-situ by XAS, using a reference sample with coverage determined by XPS. Furthermore, the chemical integrity and the coverage of the deposited LnPc<sub>2</sub> molecules were verified ex-post by XPS [see ref 18] and by STM investigations (see SI).

Circularly and linearly polarized XAS measurements at the Ln- $M_{4,5}$  and N-K absorption edges were performed in total electron yield mode. For all measurements, the base pressure in the measurement chamber was  $1.0 \times 10^{-10}$  mbar and the base temperature was 2K (BOREAS) and 8K (ID32). XMCD measurements were taken with the photon beam and the external magnetic field B (always collinear) applied either at normal and grazing incidence, that is at an angle  $\theta$  equal to 0° and 70°, respectively, relative to the surface normal (fig.1d). To avoid beam-induced molecules degradation, we minimized both the power and energy densities, respectively by defocusing the beam and regularly changing the spot position on the sample. Furthermore, we carefully monitored the XAS spectra lineshape, finding no indication of damaging.

The dichroic signal (XMCD) is a measure of the magnetization component along the impinging beam direction of the particular chemical species. It is expressed in percentage, that is by taking the difference between the two XAS spectra obtained with different x-ray polarizations ( $\sigma^{\uparrow\downarrow} - \sigma^{\uparrow\uparrow}$ ) and dividing it by the edge height of the absorption spectrum obtained by the average of the two polarizations. Notice that by defining the value of the dichroic signal in this way, it does not depend on molecular coverage.

In this work, we focus our attention on the low magnetic field behaviour of the LnPc<sub>2</sub> species: in order to get a suitable signal to noise ratio, XMCD data are obtained by integrating over several XAS acquisitions, taken at the two opposite polarizations.

The full-range magnetization curves  $M(\mathbf{B})$  (from -5 T to 5 T and the way back), taken for both Ln ions deposited on the bare Ni(111) and on SLG/Au/Ni(111) substrates (Fig.4 and Fig.S6) were obtained by plotting the maximum value of the XMCD signal as a function of the external applied magnetic field in isothermal conditions. Measurements in the low-field region [-0.5, 0.5 T] were taken in this specific range after having applied the procedure for minimizing the residual field of the magnet. In order to obtain a satisfactory S/N ratio, for the lowest field values we had to average several tens of spectra for each polarization. This implied a very long time for the acquisition in this field range, allowing us to collect only one way, i.e. from -0.5 to 0.5 T. The time required for the whole XMCD measurements in this range was about ten hours.

Conversely, in the case of SLG/Ni(111) substrate (Fig 4e,f) and for Ni(111) clean (Fig 4a,b) Ni magnetization curves were measured in a faster way, acquiring, for each field, the XAS intensities at the pre-edge (P) and at the energy corresponding to the XMCD maximum (E), and evaluating the quantity :

$$M = [(E\sigma^{\uparrow\downarrow} - P\sigma^{\uparrow\downarrow}) - (E\sigma^{\uparrow\uparrow} - P\sigma^{\uparrow\uparrow})] / 1/2[(E\sigma^{\uparrow\downarrow} - P\sigma^{\uparrow\downarrow}) + (E\sigma^{\uparrow\uparrow} - P\sigma^{\uparrow\uparrow})]$$

## Result and Discussion

### System characterization

Linearly polarized X-ray absorption measurements, performed at the N-K, Tb-M<sub>5</sub> and Er-M<sub>5</sub> edges for the two LnPc<sub>2</sub> molecules deposited on SLG/Au/Ni(111) provide us with information on the molecular adsorption geometry. As shown in Fig. 1, the dependence of the spectrum



lineshapes upon light polarization resembles that of  $\text{LnPc}_2$  deposited directly on  $\text{Ni}(111)$  Ref[13] and on  $\text{SLG}/\text{Ni}(111)$  Ref[18], proving that also in this case the  $\text{LnPc}_2$  molecules lay flat on the surface, as depicted in panel d.

Typical XAS and X-ray Magnetic Circular Dichroic (XMCD) spectra are shown in Fig. 2 and Fig.3. The lineshape of both XAS and XMCD spectra at the  $\text{Ln}-M_5$  edge for the two  $\text{LnPc}_2$  molecules deposited on  $\text{SLG}/\text{Au}/\text{Ni}(111)$  (fig.2c) is very similar to that of the corresponding ones obtained with the derivatives deposited on  $\text{SLG}/\text{Ni}(111)$  [18] (fig.2b) or directly on  $\text{Ni}(111)$  [13] (fig.2a) and does not change with temperature and magnetic field intensity (Fig.S4). This allows us to assume the integrity of the adsorbed molecules on all considered substrates.

### XMCD measurements and magnetization curves

As shown in Fig.3, where the XMCD spectra taken at high field are displayed, the intensity of the dichroic signal strongly depends on the angle  $\theta$  between the surface and the applied magnetic field. On both  $\text{SLG}/\text{Ni}(111)$  and  $\text{SLG}/\text{Au}/\text{Ni}(111)$  substrates, the high-field Tb dichroism is more intense at  $\theta=0^\circ$  than at grazing angle ( $\theta=70^\circ$ ), whilst the opposite occurs for Er, consistently with what reported in Ref. 13 and Ref. 18 for the case of bare  $\text{Ni}(111)$  and  $\text{SLG}/\text{Ni}(111)$  substrates, respectively. This confirms that, for all substrates, the easy axis of the magnetization lies perpendicular to the substrate surface in the case of Tb, whereas it is parallel to the surface plane in the case of Erbium [25].

The different orientation of the molecular easy-axis allowed us to investigate the role of anisotropy in the mechanism determining the molecule-substrate magnetic coupling. To this end, the magnetic coupling between the Ln ions and the Ni substrate was studied by taking the magnetization curves  $M(B)$ , that is by measuring the maximum value of the XMCD signal as a function of the external applied magnetic field in isothermal conditions. The full-range magnetization curves (-5 T to 5 T), taken for both Ln ions and for all three possible substrates (i.e. bare  $\text{Ni}(111)$ ,  $\text{SLG}/\text{Ni}(111)$  and  $\text{SLG}/\text{Au}/\text{Ni}(111)$ ) are shown in the SI- Fig.S6.

Here, we focus our attention on the low-field region (-1T ,1T), where the Zeeman interaction is reduced and the effect of coupling is expected to become predominant. In Fig.4, the  $M(B)$  curves at  $\text{Ln}-M_5$  edge for all three substrates are reported, along with the corresponding simulated curves (see Discussion). These are compared to the magnetization curves of the corresponding substrates

taken at the Ni-L<sub>3</sub> edge: (panel (a) reports the M(B) curve measured, at  $\theta = 70^\circ$ , on the Ni(111) single crystal used for the deposition of the TbPc<sub>2</sub> molecule, while the substrate used during the experiments with the ErPc<sub>2</sub> molecule is shown in panel (b). The Ni M(B) curves slightly differ from one Ni sample to the other. At variance, we verified that they are not affected by the surface preparation, i.e. bare Ni, SLG/Ni or SLG/Au/Ni all show identical M(B) curves.

The Ni and Tb M(B) measured at normal incidence for the TbPc<sub>2</sub> deposited on bare Ni, on SLG/Ni(111) and on SLG/Au/Ni(111) are presented in Fig. S5 (see SI). We did not show the magnetization for the ErPc<sub>2</sub> since the dichroic signal, at  $\theta = 0^\circ$ , is almost zero.

When the molecules are directly deposited on Ni (panels c and d) we observe that, for small fields, the lanthanide magnetizations are opposite to **B**. Increasing further the field magnitude, a sudden change of the slope sign is observed in correspondence to the field at which the Ni magnetization starts to saturate. Finally, the Ln magnetizations become parallel with the external magnetic field and with the magnetization of the Ni substrate for large enough values of **B**. These features demonstrate the antiferromagnetic character of the coupling of the lanthanide atom to the Ni substrate, in agreement with previously reported findings [07, 13].

When the LnPc<sub>2</sub> molecules are deposited on SLG/Ni (panels e,f), though a reversed sign of the magnetization can no longer be measured, a clear change of slope of the M(B) curves at low fields is still observed. This behaviour shows that, for both molecules, antiferromagnetic coupling with the substrate is still present, though reduced by the presence of the graphene layer. This finding, which has been already reported in the case of TbPc<sub>2</sub> [18], is here proved to be valid also in the case of ErPc<sub>2</sub>.

We now focus our attention on the effects of Au intercalation between graphene and Ni. Extracting reliable XMCD intensity values at very low field, where the dichroic signal is extremely small, is actually not trivial. To this end, we developed a fitting procedure which is illustrated in details in the SI. The results of this analysis is shown in panels g,h of Fig. 4, where the main experimental finding of the present work is reported, that is the low-field magnetization curves for Tb and Er adsorbed on gold-intercalated SLG. It is observed that, while in the case of TbPc<sub>2</sub> the gold intercalation wipes out all kinds of coupling, for ErPc<sub>2</sub> the antiferromagnetic coupling between the metal ion magnetic moment and the Ni substrate persists even when they are separated by the gold-intercalated graphene.

## Discussion.

To get a more quantitative estimate of the coupling strength between the magnetic molecules and the underlying Ni substrate in Fig. 4 we superimpose the experimental data with simulated magnetization curves (shown as red lines) of the type  $\alpha B_J(B + B_{\text{eff}})$  [Ref 32 and 12], where  $B_J$  is the Brillouin function,  $B$  is the external magnetic field and  $\alpha$  is a coefficient introduced to adjust the simulated curve to the arbitrary XMCD units.  $B_{\text{eff}}$  is an effective magnetic field, representing the magnetic coupling between the lanthanide atom and the substrate. The origin of this term is usually considered to be a super-exchange type of coupling [07, 13]. However, given the tiny energy scales under consideration in this work, we cannot rule out the contribution of the Ni(111) stray field to the observed effective  $B_{\text{eff}}$  value, as we will explain in more details in the followings. In all cases,  $B_{\text{eff}}$  is assumed to be proportional to the Ni magnetization, therefore  $B_{\text{eff}}$  is defined as  $B_{\text{eff}} = \lambda M_{\text{Ni}}$ , where  $M_{\text{Ni}}$  is the Ni(111) magnetization, as measured experimentally by XMCD and normalized to its saturation value, and  $\lambda$  is the parameter related to the strength of the coupling (expressed in Tesla). The curves in Fig.4 are calculated using  $J_{\text{Tb}} = 6$ ,  $J_{\text{Er}} = \frac{1}{2}$ , temperature  $T = 8$  K and neglecting any anisotropy.

While the correct fit of the full magnetization curves would require the complete theoretical model used in previous works[7,13,18], for the low magnetic field region which is here of interest, our measured magnetization curves are essentially linear with respect to  $B$  and the agreement with the simulated  $B_J$  function is already satisfactory. Thus, this simple model allows us to evaluate the strength of the magnetic coupling. In particular, focusing on the  $\text{ErPc}_2$  behaviour, we found that the estimated strength of the antiferromagnetic coupling is  $\lambda = -0.25 \pm 0.02 \text{ T}$  in the case of the bare Ni substrate,  $\lambda =$

$-0.08 \pm 0.02 \text{ T}$  in the case of the SLG/Ni substrate and  $-0.08 \pm 0.02 \text{ T}$  when  $\text{ErPc}_2$  molecules are deposited on Au-intercalated SLG on Ni(111).

Instead, in the case of the  $\text{TbPc}_2$  we found  $\lambda = -0.9 \pm 0.02 \text{ T}$  when  $\text{TbPc}_2$  molecules are deposited directly on Ni,  $-0.1 \pm 0.02 \text{ T}$  on the SLG/Ni substrate and zero for SLG/Au/Ni(111). Here the minus sign accounts for the antiferromagnetic nature of the coupling.

We should here mention that, at variance with measurements performed at grazing incidence ( $\theta=70^\circ$ ), the TbPc2/SLG/Ni M(B) measurements at  $\theta=0^\circ$  (see SI) does not show any signature of molecule/substrate magnetic coupling. This can be explained considering the angular dependence of the Nickel magnetization curves: while at  $\theta=70^\circ$  Ni magnetization saturates already at  $\sim 0.2$  T, at  $\theta=0^\circ$  saturation occurs only for magnetic field values  $> 0.5$  T. Therefore, at  $\theta=0^\circ$  and for fields smaller than 0.5 T, which is the relevant case here, Ni magnetization is significantly smaller than its saturation value, thus substantially hampering the experimental observation of the possible magnetic coupling signature.

The effect of introducing a graphene layer between the molecule and the ferromagnetic Ni(111) substrate has been already discussed in details in our recent work in the case of TbPc2[18]. Graphene directly grown on Ni still allows magnetic coupling, although a substantial weakening is observed. The intercalation of a Au layer makes the coupling between the Tb magnetic moment and the Ni substrate no more detectable within our experimental accuracy.

The situation is quite different in the case of ErPc2, where the gold intercalation has essentially no effect on the coupling. It is worth to remark here the different relative orientation of the magnetic anisotropy of the two Ln ions (easy-axis for Tb vs easy-plane for Er) and the Ni substrate magnetization. Indeed, the critical role of the alignment between the molecular easy axis and the substrate magnetization has been already demonstrated in the case of TbPc2 on Ni thin films [07].

Starting from these considerations, we can envisage a qualitative explanation for the observed behaviour, which takes into account the dipolar stray field coming from the magnetization of the nickel substrate. A precise evaluation of the intensity of the substrate-induced stray field would require a detailed knowledge of closure-domain distribution at the surface, which is indeed a demanding issue. Nonetheless, the order of magnitude of the magnetic field intensity at the nickel surface, produced by the uniform magnetization of the whole (macroscopic) crystal can be estimated calculating the field produced by a uniform collection of magnetic dipoles, each of which is associated to a single atom of the Ni sample (see details of the calculations in the ESI).

The magnetic field components perpendicular ( $B_z$ ) and parallel ( $B_x$ ) to the surface of a disc-shaped sample of radius  $R$  and thickness  $D$ , calculated along its axis, at a distance  $d$  from the surface, are given by:

$$B_x(0, d) = -\frac{\mu_0 \mu_B}{4\pi V_{cell}} \sin(\alpha) \left[ \frac{-\pi d}{\sqrt{R^2 + d^2}} + \frac{\pi(D+d)}{\sqrt{R^2 + (D+d)^2}} \right] \xrightarrow{d \ll D} -\frac{\mu_0 \mu_B}{4\pi V_{cell}} \sin(\vartheta) \left[ \frac{\pi D}{\sqrt{R^2 + D^2}} \right] \quad (1)$$

$$B_z(0, d) = \frac{\mu_0 \mu_B}{4\pi V_{cell}} \cos(\alpha) \left[ \frac{-2\pi d}{\sqrt{R^2 + d^2}} + \frac{2\pi(D+d)}{\sqrt{R^2 + (D+d)^2}} \right] \xrightarrow{d \ll D} \frac{\mu_0 \mu_B}{4\pi V_{cell}} \cos(\vartheta) \left[ \frac{2\pi D}{\sqrt{R^2 + D^2}} \right] \quad (2)$$

These results show that the strength of the dipolar field at the surface depends critically on the aspect ratio  $D/R$  and is therefore non-negligible in the case (as ours) of macroscopically thick samples. Moreover and most importantly, they demonstrate that the intensity of the dipolar magnetic field does not depend on the distance  $d$  from the nickel surface, as long as  $d \ll D$  (i.e.  $d$  is in the nm range, while  $D$  is in the mm range).

Upon inserting the values of the Bohr magneton  $\mu_B$ , the Nickel unit cell volume  $V_{cell}$  and the sample dimensions  $D$  and  $R$  in eqq. (1-2), we obtain that the magnitude of both components is of the order of tens of mT, ( $B_x = -50$  mT and  $B_z = +35$  mT), i.e. the same as the coupling strength previously experimentally evaluated.

It is important here to note that the component parallel to the surface is more intense than the orthogonal one. Furthermore, the first is negative, i.e. it would provide an anti-ferromagnetic coupling (with respect to the Ni magnetization) with a magnetic dipole located at the surface, whereas the latter is positive, i.e. it would induce a ferro-magnetic coupling. The dipolar field felt by the adsorbed molecules is therefore not negligible and essentially the same independently from the layers (SLG, Au) under them. On the contrary, the (super-) exchange interaction, being mediated by wave-functions, strongly depends on distance and/or interposed layer. In previous works we proved that SLG was able to keep a significant exchange coupling between Ni and the lanthanide atom. This is true in particular for Tb, which also shows the strongest coupling among the studied lanthanide species. The vanishing of the coupling when gold is intercalated suggests the vanishing of the exchange interaction responsible for the coupling.

So, why does Er keep the same coupling as without gold? Possibly, the coupling of the Er atoms is mainly due to the dipolar field already for the case of the SLG/Ni(111) substrate, and this would come from its in-plane anisotropy, favouring the coupling with the in-plane dipolar field. The invariance of the coupling strength with or without the gold layer is a strong clue in this direction. Of course a similar interaction is present also for Tb, but the coupling between the in-

plane dipolar field and the easy-axis anisotropy, orthogonal to it, makes the coupling too weak to be detected.

In conclusion, we have studied the magnetic coupling between two types of  $\text{LnPc}_2$  molecules, characterized by different magnetic anisotropies, and a Ni(111) magnetic substrate through an Au-intercalated SLG layer. In the case of Tb, the antiferromagnetic signal – which can be attributed to (super)-exchange coupling, vanishes upon Au intercalation. This effect can be attributed to both the increased distance between the molecular species and the magnetic substrate and to the same mechanisms leading to the intercalation-induced electronic decoupling of the graphene layer from the Ni substrate. A full understanding of the mechanisms underlying the observed vanishing would require a detailed theoretical modelling of the system, which implies considerable computational efforts and is clearly beyond the scopes of this work.

In the case of Er on the other hand, the small antiferromagnetic signal does not seem to be affected by intercalation, which can be rationalized taking into account a relevant contribution of the substrate magnetic dipolar field. Our work therefore suggests the possible importance of the magnetic dipolar field in determining the behaviour of hybrid metal-organic magnetic interfaces, especially when combined with the magnetic anisotropy of the systems.

### Acknowledgements.

This work was partially supported by European Community through the FET-Proactive Project MoQuaS by contract no. 610449 and by the Italian Ministry for Research (MIUR) through the PRIN grant 20105ZZTSE “GRAF” and through the Futuro In Ricerca (FIR) grant RBFR13YKWX. We acknowledge the ESRF, ALBA and ELETTRA Synchrotron facilities and their beamline staffs for assistance in XAS experiments (beamlines ID32 and BOREAS) and ARPES (APE beamline).

## References

- [01] L. Bogani, W. Wernsdorfer, *Nat Mater*, 2008, **7**, 179.
- [02] S. Sanvito, *Chem. Soc. Rev.*, 2011, **40**, 3336.
- [03] Y. Lan, S. Klyatskaya, M. Ruben, O. fuhr, W. Wernsdorfer, A. Candini, V. Corradini, A. Lodi Rizzini, U. del Pennino, F. Troiani, L. Joly, D. Klar, H. Wende and M. Affronte, Magnetic interplay between two different lanthanides in a tris-phthalocyaninato complex: a viable synthetic route and detailed investigation in bulk and on surface, *J. Mater. Chem. C*, 2015, **3**, 9794-9801.
- [04] A. Cornia, D. Taham, M. Affronte, *Thin layers of Molecular Nanomagnets, chapter 8 (p.187-230) in book Molecular Magnetic Materials. Concepts and applications. Ed. Barbara Sieklucka and Dawid Pinkowicz Wiley* (2016) ISBN: 978-3-527-33953-2
- [05] A. Scheybal, T. Ramsvik, R. Bertschinger, M. Putero, F. Nolting, and T. A. Jung, *Chem. Phys. Lett.*, 2005, **411**, 214.
- [06] Wende et al., *Nat. Mater.*, 2007, **6**, 516.
- [07] A. Lodi Rizzini et al., *Phys. Rev. Lett.*, 2011, **107** (17), 177205.
- [08] S. Javaid, M. Bowen, S. Boukari, L. Joly, J. -B. Beaufrand, X. Chen, Y. J. Dappe, F. Scheurer, J. -P. Kappler, J. Arabski, W. Wulfhekel, M. Alouani, and E. Beaurepaire, *Phys. Rev. Lett.*, 2010, **105**, 077201.
- [09] E. Annese, J. Fujii, I. Vobornik, G. Panaccione, G. Rossi, *Phys. Rev. B*, 2011, **84**, 174443.
- [10] N. Ishikawa, M. Sugita, T. Ishikawa, S. Koshihara, and Y. Kaizu, *J. Am. Chem. Soc.*, 2003, **125**, 8694.
- [11] N. Ishikawa, M. Sugita, T. Ishikawa, S. Koshihara, and Y. Kaizu, *J. Phys. Chem. B*, 2004, **108**, 11265.
- [12] A. Candini, V. Bellini, D. Klar, V. Corradini, R. Biagi, V. De Renzi, K. Kummer, N. Brooks, U. del Pennino, H. Wende, M. Affronte, Ferromagnetic Exchange Coupling between Fe Phthalocyanine and Ni(111) Surface Mediated by the Extended States of Graphene, *J. Phys. Chem. C*, 2014, **118**, 17670.
- [13] A. Candini, D. Klar, S. Marocchi, V. Corradini, R. Biagi, V. de Renzi, U. del Pennino, F. Troiani, V. Bellini, S. Klyatskaya, M. Ruben, K. Kummer, N. B. Brookes, H. Huang, A. Soncini, H. Wende, M. Affronte, Spin-communication channels between Ln(III) bis-phthalocyanines molecular nanomagnets and a magnetic substrate, *Scientific Reports*, 2016, **6**, 21740.
- [14] A. Barla et al., *ACS Nano*, 2015, **10** (1), 1101.
- [15] Hermanns et al., *Adv. Mater.*, 2013, **25** (25), 3473.



- [16] S. Bhandary, O. Eriksson, and B. Sanyal, *Sci. Rep.*, 2013, **3**, 3405.
- [17] D. Klar, S. Bhandary, A. Candini, L. Joly, P. Ohresser, S. Klyatskaya, M. Schleberger, M. Ruben, M. Affronte, O. Eriksson, B. Sanyal, and H. Wende, *Phys. Rev. B*, 2014, **89**, 144411.
- [18] S. Marocchi, A. Candini, D. Klar, W. Van den Heuvel, H. Huang, F. Troiani, V. Corradini, R. Biagi, V. De Renzi, S. Klyatskaya, K. Kummer, N. B. Brookes, M. Ruben, H. Wende, U. del Pennino, A. Soncini, M. Affronte, and V. Bellini, Relay-Like Exchange Mechanism through a Spin Radical between TbPc2 Molecules and Graphene/Ni(111) Substrates, *ACS Nano*, 2016, **10**, 9353-9360.
- [19] N. Tombros, C. Jozsa, M. Popinciuc, H. T. Jonkman, and B. J. van Wees, *Nature*, 2007, **448** (7153), 571.
- [20] A. K. Geim and K. S. Novoselov, *Nature Materials*, 2007, **6**, 183.
- [21] T. Olsen, J. Yan, J. J. Mortensen, and K. S. Thygesen, *Phys. Rev. Lett.*, 2011, **107**, 156401.
- [22] F. Mittendorfer, A. Garhofer, J. Redinger, J. Klimeš, J. Harl, and G. Kresse, *Phys. Rev. B*, 2011, **84**, 201401(R).
- [23] A. Varykhalov, J. Sa'nchez-Barriga, A. M. Shikin, C. Biswas, E. Vescovo, A. Rybkin, D. Marchenko, and O. Rader, Electronic and magnetic properties of quasifreestanding graphene on Ni, *Phys. Rev. Lett.*, 2008, **101**, 157601.
- [24] D. Marchenko, A. Varykhalov, M.R. Scholz, G. Bihlmayer, E.I. Rashba, A. Rybkin, A.M. Shikin and O. Rader, Giant Rashba splitting in graphene due to hybridization with gold, *Nature Comm.*, 2012, **3**, 1232.
- [25] N. Ishikawa, M. Sugita, W. Wernsdorfer, Quantum Tunneling of Magnetization in Lanthanide Single-Molecule Magnets: Bis(phthalocyaninato)terbium and Bis(phthalocyaninato)dysprosium Anions, *Angewandte Chemie International Edition*, 2005, **44**, 2931.
- [26] R. Addou, A. Dahal, P. Sutter and M. Batzill, Monolayer graphene growth on Ni(111) by low temperature chemical vapor deposition, *Applied Physics Letters*, 2012, **100**, 021601.
- [27] J. Lahiri, T. S. Miller, A. J. Ross, L. Adamska, I. I. Oleynik and M. Batzill, Graphene growth and stability at nickel surfaces, *New Journal of Physics*, 2011, **13** 025001.
- [28] A. Grüneis, K. Kummer and D. V. Vyalikh, Dynamics of graphene growth on a metal surface: a time-dependent photoemission study, *New Journal of Physics*, 2009, **11** 073050.
- [29] G. Panaccione et al., *Rev. Sci. Instrum.* 2009, **80**, 043105.
- [30] A. Barla et al., *J. Synchrotron Rad.* 2016, **23**, 1507.



- [31] K. Kummer et al., *J. Synchrotron Rad.* 2016, **23**, 464.
- [32] C. F. Hermanns, K. Tarafder, M. Bernien, A. Krüger, Y.-M. Chang, P. M. Oppeneer, W. Kuch, Magnetic Coupling of Porphyrin Molecules Through Graphene, *Adv. Mater.*, 2013, **25**, 3473.

## FIGURES.

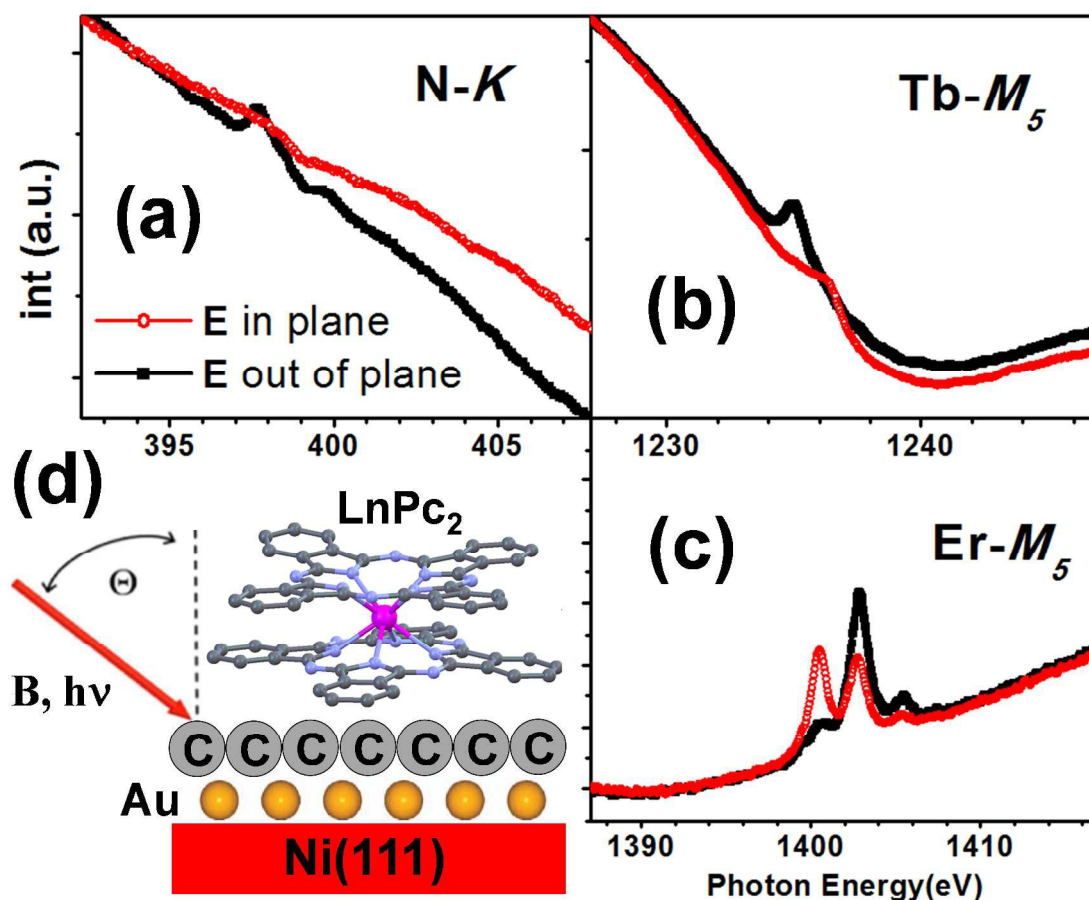


**Fig.1** XLD Linearly polarized X-ray absorption spectra at the N-K (a), at the Tb-M<sub>5</sub> (b) and Er-M<sub>5</sub> (c) edge for the LnPc<sub>2</sub> on SLG/Au/Ni(111) measured at grazing angle ( $\theta = 70^\circ$ ) at  $T = 2\text{K}$ . (d) Sketch of the measuring conditions with the LnPc<sub>2</sub> molecule lying flat on the Ni(111)/Au/SLG surface. The magnetic field **B** and the x-ray beam are collinear and oriented at an angle  $\theta = 70^\circ$  with respect to the normal to the surface. The X-ray linear polarization is chosen for having the electric field either parallel to the sample surface plane or turned  $90^\circ$  from it, that is lying in the incidence plane.

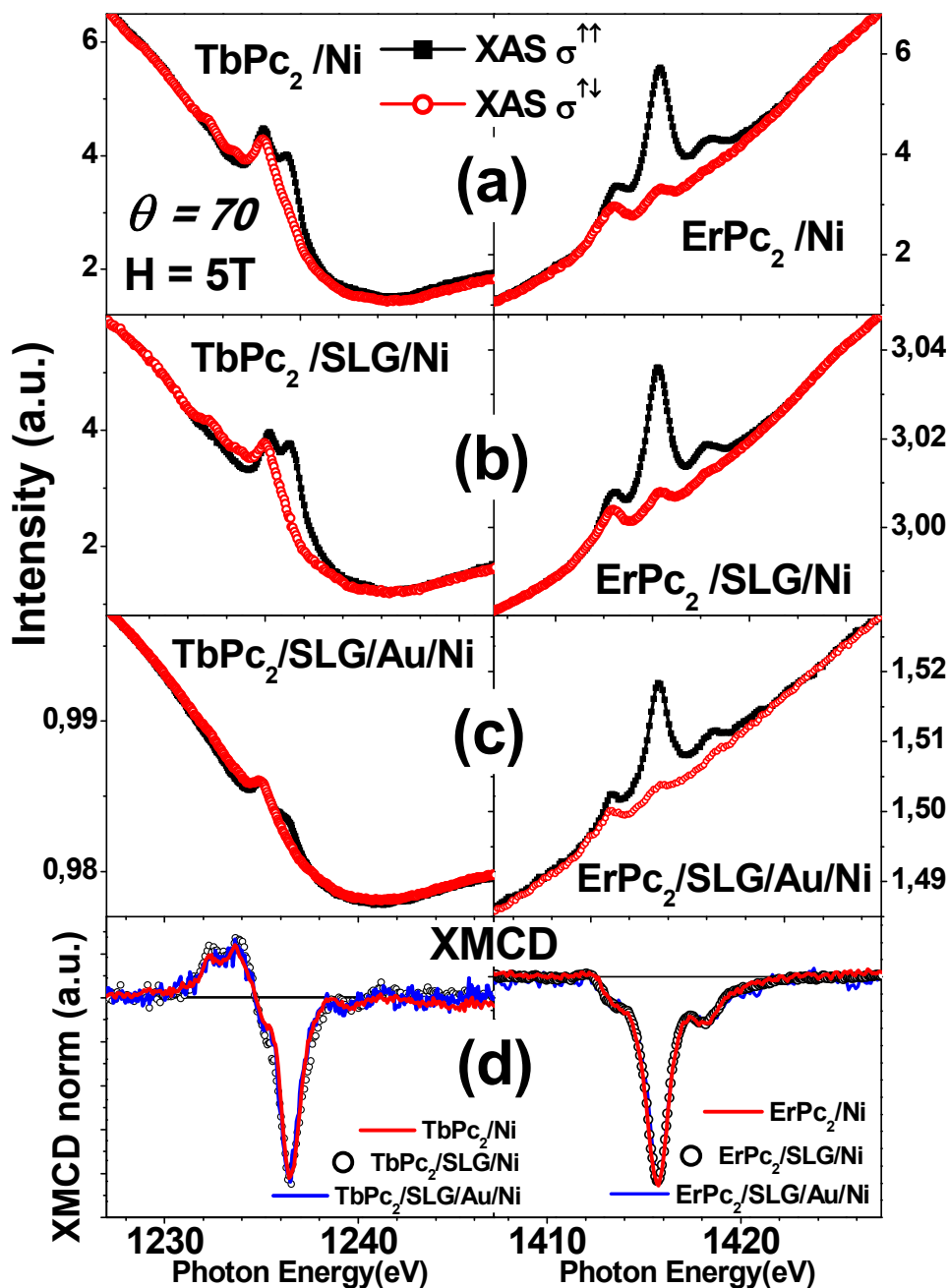


**Fig.2** Comparison of the XAS spectra at the Ln  $M_5$  edge for the  $\text{LnPc}_2$  on  $\text{SLG}/\text{Au}/\text{Ni}(111)$  (panel c) with the corresponding ones obtained on bare  $\text{Ni}(111)$  (a) and on  $\text{SLG}/\text{Ni}(111)$  (b). The data relative to the  $\text{LnPc}_2$  molecules deposited on bare  $\text{Ni}(111)$  [13] and for the  $\text{TbPc}_2$  on  $\text{SLG}/\text{Ni}(111)$  [18] are taken from our previous works and shown for comparison. The shape of the XMCD spectra (d) is the same for the three substrates. Measurement conditions:  $H = 5\text{T}$ ,  $\theta = 70^\circ$ . Temperature is  $T = 8\text{K}$  for panels a and b and  $T = 2\text{K}$  for panel c.

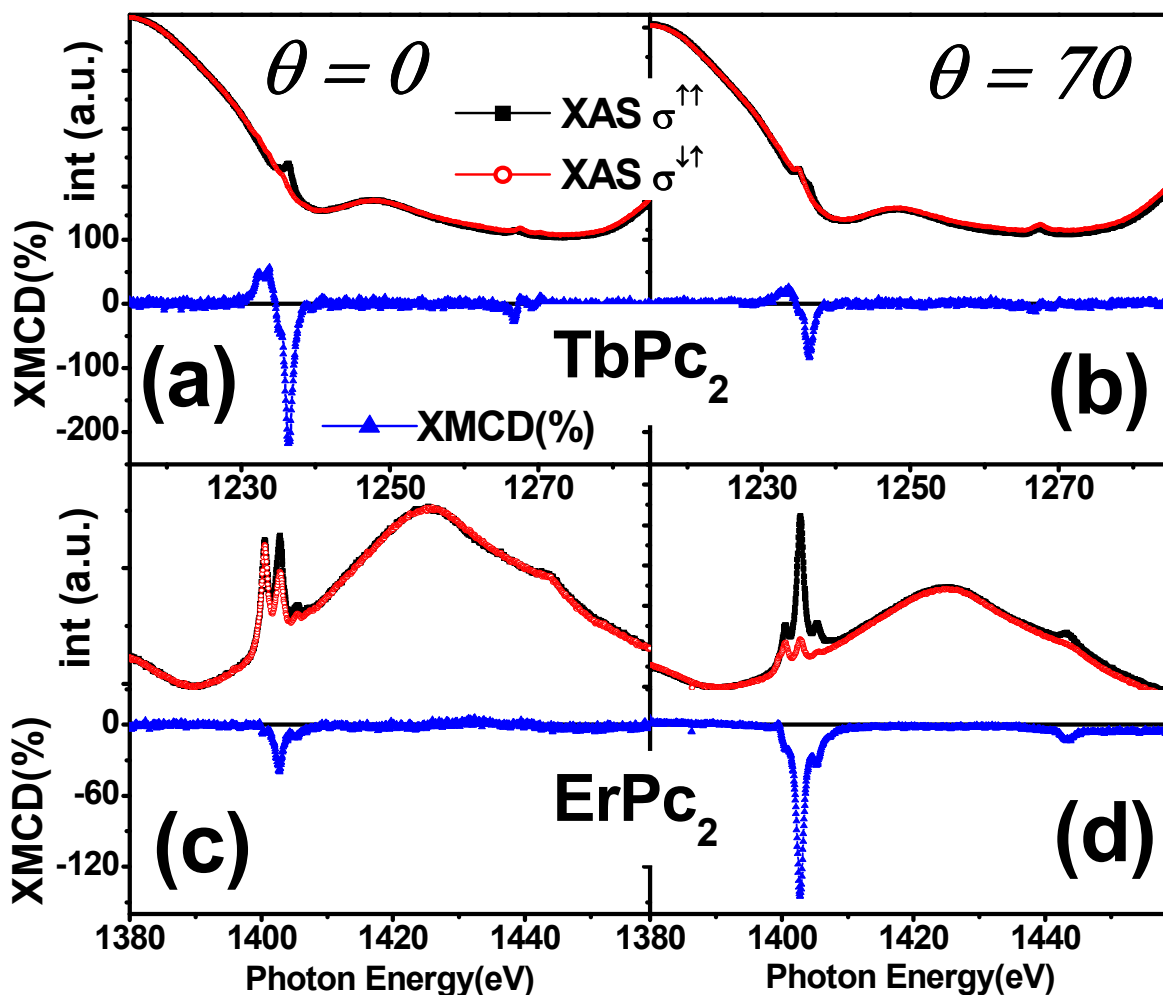


**Fig.3** Absorption spectra taken with  $\sigma^{\uparrow\downarrow}$  and  $\sigma^{\downarrow\uparrow}$  circularly polarized light (upper spectra in each panel) and the relative XMCD  $(\sigma^{\uparrow\downarrow} - \sigma^{\downarrow\uparrow}) / (\sigma^{\uparrow\downarrow} + \sigma^{\downarrow\uparrow})/2$  (lower spectra in each panel) at the Ln-  $M_{4,5}$  edges for LnPc<sub>2</sub> [Tb (a,b), and Er (c,d)] on SLG/Au/Ni(111) at  $\vartheta = 0^\circ$  (left panels) and  $\vartheta = 70^\circ$  (right panels) incidence angles, taken at an applied external field  $B = 5\text{ T}$  and  $T = 2\text{ K}$ .

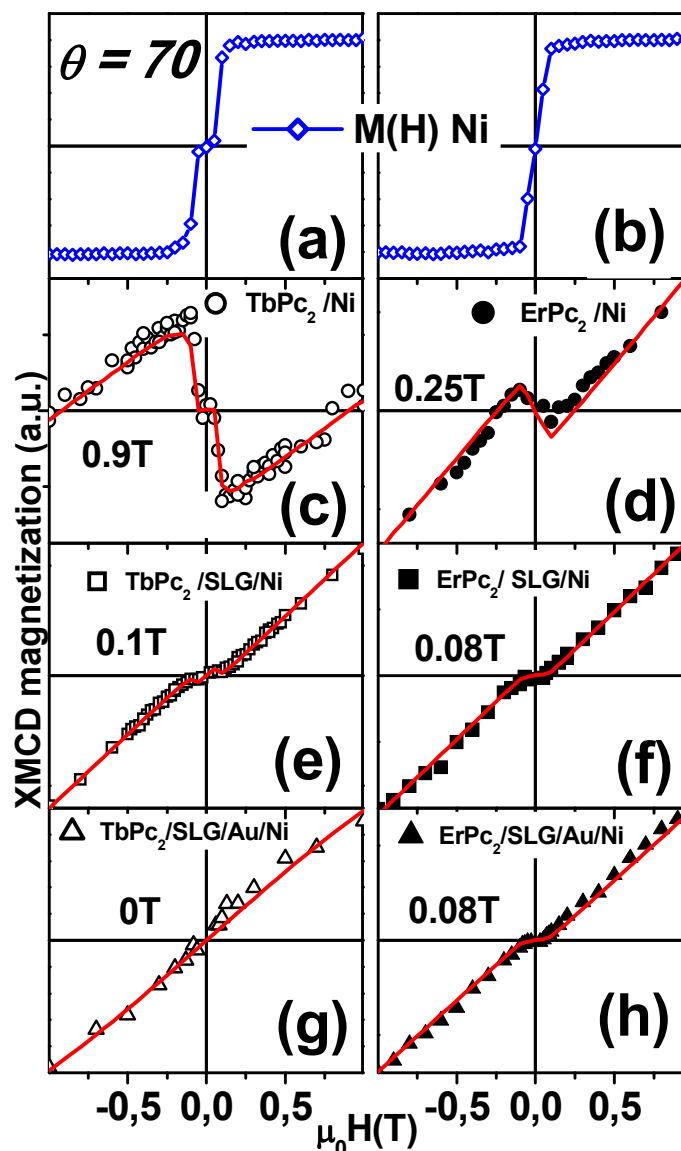


**Fig.4** Comparison between the magnetization curves at the Ni- $L_3$  (panels a and b) and at the Ln- $M_{4,5}$  edges (Tb left panels and Er right panels) at  $\vartheta = 70^\circ$ . The hysteresis of the two Ni are different because the measurements on TbPc<sub>2</sub> and ErPc<sub>2</sub> were performed on two different Ni(111) single crystals. The experimental curves (symbols in panels c-h) are in excellent agreement with the simulated ones (red lines) as described in the text. The Ln data are a low-field magnification of Figure S6. Data from panels c, d and e are taken from references [13 and 18], respectively. In bold we indicate the values of the exchange strength ( $\lambda$ ), expressed in Tesla. The temperature is 8K for all the measurements apart in panel g, measured at T 2K.

